Effect of Secondary Explosive Welding on Microstructure and Mechanical Properties of 10CrNi3MoV Steel-Based Composite Plates

CHANGQING YE, WEIGUO ZHAI, GUANGYAO LU, QINGSONG LIU, LIANG NI, LIANG YE, and XIAO FANG

The secondary explosive welding process promotes the diffusion of the carbon element and accumulation of chromium carbide, which leads to a decrease of tensile properties and toughness of the material. In this work, the average shear strength value increased from 400 to 421 MPa. The crack of the fatigue specimens started from the inclusions rich in alumina near the surface, and the harmful hard-phase inclusions were exposed because of stress concentration. The maximum load limit of 10CrNi3MoV steel undergoing secondary explosive welding was between 590 and 605 MPa.

https://doi.org/10.1007/s11661-021-06190-z

COMPOSITE plates can effectively solve the issue of commonly used homogeneous metal materials not being able to meet the demand for high output in industry.[1,2] Composite plates have better metallic properties and unparalleled comprehensive performance and therefore have continuously satisfied the increasing demands for outstanding functional and structural materials in chemical vessels, shipbuilding and nuclear industries.[3–6] The stainless steel 304L (SS304L) and the high-strength low-alloy (HSLA) 10CrNi3MoV steel composite plates (or sandwich structure SS304L/steel/SS304L) studied in this work have broad application prospects in pressure-bearing and anti-corrosion equipment. The reason is that they can combine the excellent corrosion resistance of SS304L with low carbon content and the high strength and low temperature high toughness of 10CrNi3MoV steel. The research and development of the large-area SS304L/10CrNi3MoV steel composite plates originated from the design and construction of a new type of small offshore nuclear reactor, which is supposed to be installed on ships and could operate at sea providing sufficient electric power for users in need. In the design of the structure of the suppression pool in a nuclear reactor, the designers are faced with complex material selection issues. There is an urgent need for structural materials with high strength and toughness as well as excellent water corrosion resistance. In this field of research, explosive welding is a potential solid-state method applied to fabricate large-area SS304L/10CrNi3MoV steel composite plates, which are difficult to join by conventional methods because of potential technical difficulties such as metallurgical incompatibility.[7–10] Explosive welding technology employs the huge energy of detonation to achieve the bonding between two different types of metal plates. Because of its simple process and low loss, it is usually considered a relatively versatile manufacturing method.[11,12] The pressure generated by this collision will cause excessive plastic deformation at the interface and mix the surface layers of the materials so that they bond together, thereby forming a linear or wavy interface in an explosive welded joint. During the explosion, the upper flyer plate primarily bends and then collapses on the bottom plate, and a heated gas jet is formed between these two plates to clean their surfaces for bonding together. The explosive welded interface plays an important role in the eventual characteristics of the composite plates. The formation of intermetallic compounds, interface structure, local melting and adhesion strength are all metallurgical and mechanical interface characteristics, and they dominate the overall performance of explosive welded composite plates.[13–15] Considering the SS304L/steel/SS304L sandwich structure obtained by the secondary explosive welding process, it is necessary to study the effect of the process on the interface characteristics and overall performance of the composite plates. The aim of present work is to relate the

CHANGQING YE, GUANGYAO LU, QINGSONG LIU, LIANG NI, and LIANG YE are with the China Nuclear Power Technology Research Institute Co., Ltd., Shenzhen, 518026, China. WEIGUO ZHAI is with the Luoyang Ship Material Research Institute, Luoyang, 471023, China. XIAO FANG is with the Sino-French Institute of Nuclear Engineering and Technology, Sun Yat-sen University, Zhuhai, 519082, China. Contact e-mail: fangx26@mail.sysu.edu.cn

Manuscript submitted September 26, 2020; accepted February 6, 2021.

Article published online March 4, 2021

secondary explosive welding process to the interfacial microstructure features and the mechanical properties of the 10CrNi3MoV steel-based composite plates. The composite plates manufactured using the technique described herein will be able to solve the above-mentioned structural material demand problem.

In the fabrication of SS304L/10CrNi3MoV steel or SS304L/10CrNi3MoV steel/SS304L composite plates, as illustrated in Figures 1(a) and (b), the flyer layer (SS304L: 0.03 wt pct C, 19.06 wt pct Cr, 9.28 wt pct Ni, 1.78 wt pct Mn, 0.54 wt pct Si) with dimensions of 4 mm × 1500 mm × 7000 mm and the base material (10CrNi3MoV steel: 0.08 wt pct C, 0.92 wt pct Cr, 2.89 wt pct Ni, 0.47 wt pct Mn, 0.24 wt pct Si) with dimensions of 32 mm × 1500 mm × 7000 mm were arranged in a parallel scheme. The explosive material was an ammonium nitrate expanded with a mixture of inert additives as described in a previous work.[16] After one explosive welding, a single-layer SS304L composite plate was obtained through heat treatment and leveling procedures to release the residual stress of the explosive welding and restore the performance of the material, as shown in Figure 1(a). The heat treatment was operated at 645 °C for 240 minutes followed with air cooling. A double-layer SS304L composite plate was realized by using an entire single-layer SS304L composite plate as the base metal, and then the free surface of another piece of 10CrNi3MoV steel was welded to the second SS304L flyer plate by the secondary explosive welding. Then, the same heat treatment and leveling process was applied to the double-layer SS304L composite plate. The two interfaces formed in the double-layer SS304L composite plates were interface A (Figure 1(b)), which had undergone two explosive welding processes, and interface B (Figure 1(b)), which had undergone only one explosive welding process. In addition, an improper high-temperature heat treatment process may cause chromium carbides to precipitate at grain boundaries, resulting in sensitization of austenitic stainless steel, thereby reducing the intergranular corrosion resistance.[17] The explosively welded SS304L was tested for intergranular corrosion according to the ASTM A262 standard. All the specimens were bent to 180 degree, and no cracks on the outer surface caused by intergranular corrosion were observed. The secondary explosive welding process did not affect the functional design goal of SS304L for corrosion resistance.

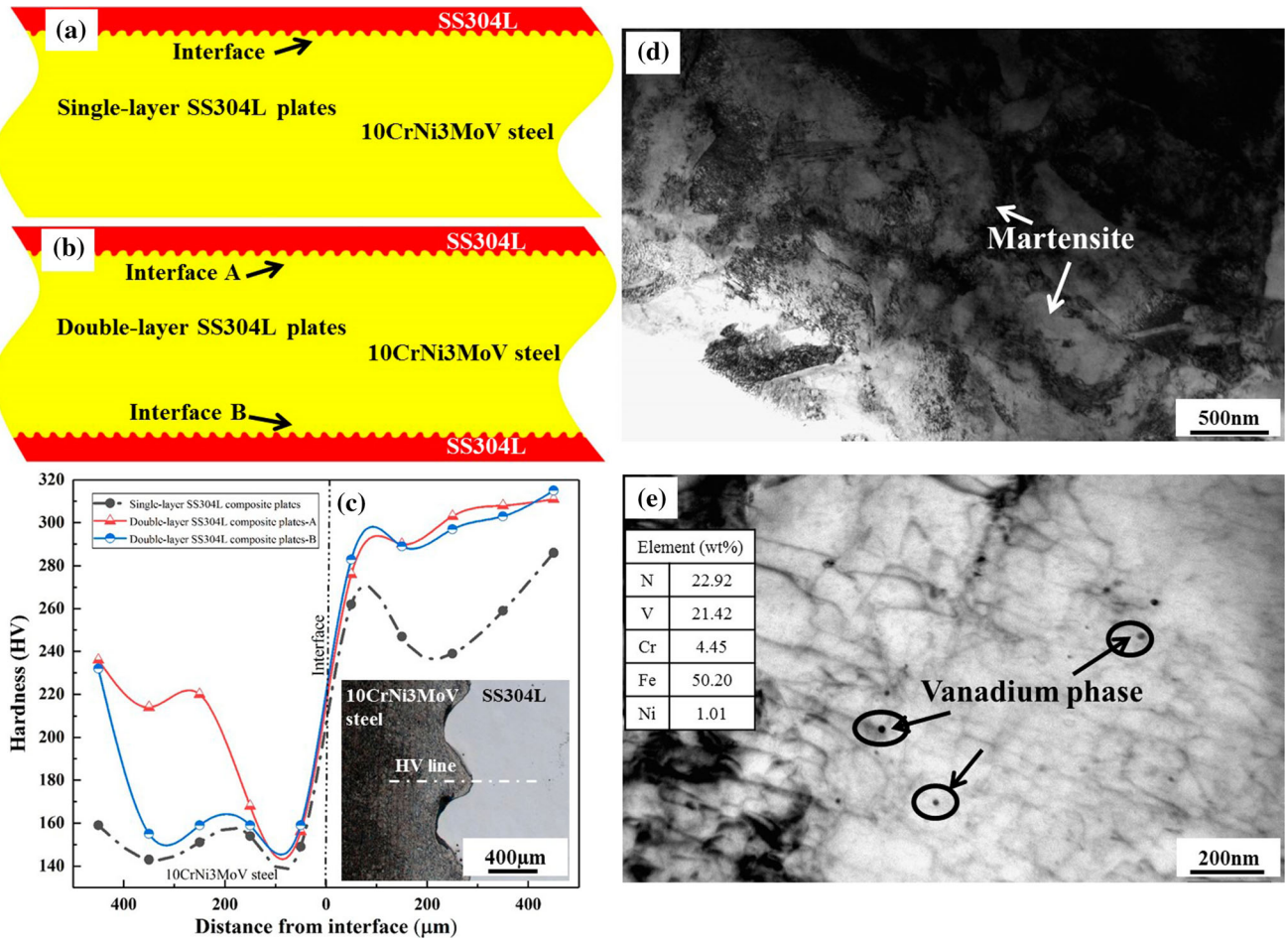

Fig. 1—(*a*) Schematic diagram of the single-layer SS304L composite plates; (*b*) schematic diagram of the double-layer SS304L composite plates with a secondary explosive welding process; (*c*) Vickers hardness value profile; (*d*) TEM microstructure of the interface near SS304L; (*e*) TEM microstructure of the interface near 10CrNi3MoV steel.

Transmission electron microscopy (TEM) was used to analyze the microstructures of the hardened specimens. Microstructures and distributions of phases were observed using scanning electron microscopy (SEM) and electron backscattered diffraction (EBSD). The distribution of the alloy element along the explosive welding interface was carried out by electron probe microanalyses (EPMA). To evaluate the impact of the secondary explosive welding process on the mechanical properties of the composite plates, hardness measurements, tensile tests, impact tests, shear tests and fatigue tests were performed. Microhardness tests were carried out under a load of 100 g for 10 seconds. The functional SS304L layer was removed, and the tensile and impact specimens were made of 10CrNi3MoV steel, which was the main load-bearing and compressive base material. Round tensile specimens of 10 mm diameter, 60 mm gauge length and 100 mm total length were employed. Charpy V-notch specimens with dimensions of 55 mm × 10 mm × 10 mm were tested at − 20 °C. Specimens for shear tests were prepared parallel to the explosion direction based on the Chinese standard GB/T6396-2008.[18] At least three specimens were tested under the same condition, and average values were calculated. In addition, to obtain the effect of the secondary explosive welding process on the number of load cycles required for the fracture of 10CrNi3MoV steel, a fatigue test was carried out at room temperature under given load and frequency conditions. The termination of a fatigue specimen referred to failure of the specimen or load cycle reaching 2×10^6 times. The stress ratio of a fatigue test was 0.1, and the loading frequency was 133 Hz. A fatigue specimen with a gauge length of 25 mm, gauge length of 5 mm and total length of 126 mm was prepared.

After explosive welding, the chemical composition and microstructure of the dissimilar material interfaces have changed significantly, depending on the properties of the two materials and the welding process. The measurement results of the microhardness across the interface of the explosive welded composite plates are shown in Figure 1(c). The average microhardness values and standard deviations of the two materials in the initial state were 237 ± 3 and 213 ± 3 HV, respectively, corresponding to 10CrNi3MoV steel and SS304L. The microhardness of SS304L in the double-layer SS304L composite plates increased by about 32 pct (311 HV). In the single-layer SS304L composite plates, the microhardness of SS304L increased by about 26 pct (286 HV). The hardness of the SS304L layer side adjacent to the interface was significantly enhanced because of the strain hardening caused by the explosive welding. The microhardness profile in Figure 1(c) reveals a sharp decrease in the bonding zone, especially in the interface near 10CrNi3MoV steel, because of the carbon diffusion loss. At distances away from the interface, an increase of microhardness was observed until it approached the original hardness in 10CrNi3MoV steel. The secondary explosive welding process improved the hardness of the area near the interface, which was most significant at interface A in 10CrNi3MoV steel. The increase probably arises from the balance between the explosive strain hardening and heat treatment softening processes.[3,16,19] During the explosive welding process, martensite was formed because of shear deformation at a distance of 50 μm from the SS304L zone near the interface, and the high-hardness vanadium-containing phase in steel consolidated the hardening effect, which was confirmed by TEM examination as shown in Figures 1(d) and (e).

Figure 2 shows the optical image of the interface in explosively bonded SS304L/10CrNi3MoV steel composite plates without heat treatment. Under the action of explosive welding, the interface metals were seriously deformed, and the crystal grains were elongated as shown in Figure 2.

Figure 3 shows the microstructure, crystal orientation and phases on the original materials, and the cross section of SS304L/10CrNi3MoV steel interfaces experienced heat treatment obtained by SEM and EBSD. The interface zone comprised five phases: austenite, ferrite, $Cr_{23}C_6$, Cr_7C_3 and Fe_3C. As shown in Figures 3(a) through (f), the main microstructures of SS304L and 10CrNi3MoV steel were austenite (FCC) and ferrite (BCC), respectively. After explosive welding, due to recrystallization under the subsequent heat treatment process, the explosively deformed grains had been restored to equiaxed grains, and interface stainless steel grains had been significantly refined (Figures 3(a), (b), (g), (h), (k), and (n)). Both single- and double-layer SS304L composite plates had typical wavy interfaces structures, including a vortex region (Figures 3(g), (j), and (m)). The findings clearly indicated that the explosive welding process promoted accumulation and growth of chromium carbides ($Cr_{23}C_6$ and Cr_7C_3). Under the action of secondary explosive welding, the amount of $Cr_{23}C_6$ increased and became coarser as shown in Figure 3(c), (f), (i), (l), and (o). The Cr_7C_3 phase dissolved and transformed into $Cr_{23}C_6$ phase.

To clarify the distributions of various alloy elements in the interface, EPMA was used to line scan elemental distributions in the vortex zone and the solid-solid bonding zone as shown in Figure 4. The interface thickness of the transition layer between SS304L and 10CrNi3MoV steel changed in the vortex zone and solid-solid bonding zone, which was caused by uneven microstructure in the interface. As illustrated in Figures 4(a) through (f), the thickness of the transition

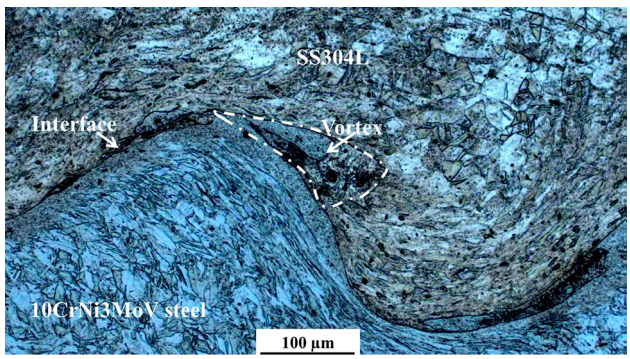

Fig. 2—Optical microscopy image of the interface in explosively bonded composite plates without heat treatment.

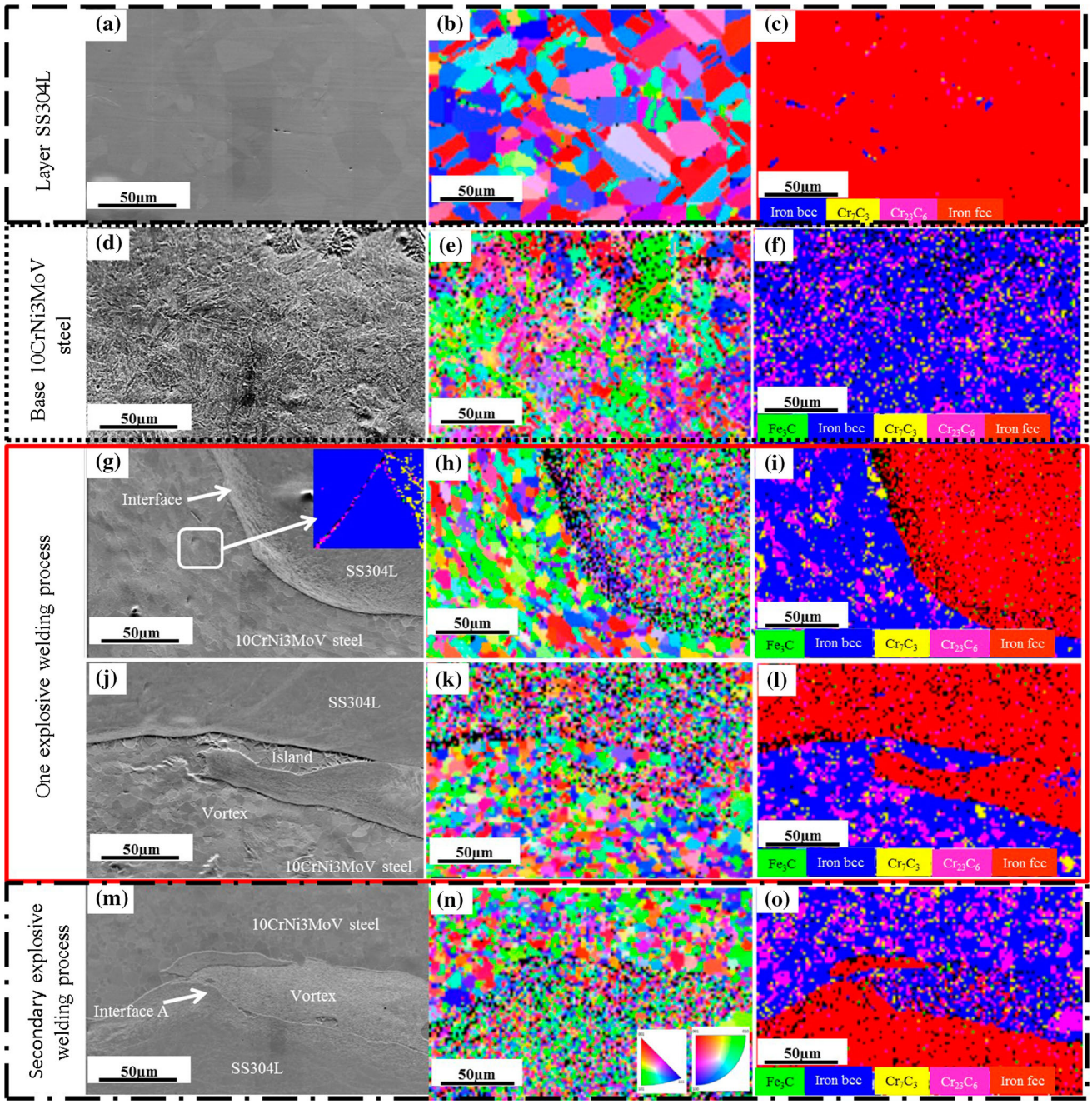

Fig. 3—SEM and EBSD results of the composite plates and the interfaces: (*a*) through (*c*) the SS304L layer; (*d*) through (*f*) the base 10CrNi3MoV steel; (*g*) through (*i*) the wave interface with one explosive welding process; (*j*) through (*l*) the interface included the vortex and experienced one explosive welding; (*m*) through (*o*) the interface included the vortex and experienced secondary explosive welding process.

layer in the vortex region was approximately 100 μm and that in the solid-solid bonding region was approximately 25 μm. Therefore, it can be inferred that there was a certain amount of melt which completely entered the materials to form a vortex area. The EPMA scan line of element C revealed several high peaks at the interface and the vortex area, which may be related to the higher diffusion rate and the lower solubility of element C in 10CrNi3MoV steel than in SS304L. This was also related to the formation of more $Cr_{23}C_6$ phase in ferrite under the effect of the high-energy detonation and subsequent heat-treatment process. The EPMA analyses matched well with those obtained by phase identification by EBSD.

The mechanical test results are summarized in Table I. The secondary explosive welding process reduced the tensile properties and the toughness of 10CrNi3MoV steel. However, the tensile strength of the 10CrNi3MoV steel was maintained at $>$ 680 MPa, and the yield strength was $>$ 600 MPa. The impact energy of the 10CrNi3MoV steel was reduced by 28 pct from 290 J to 210 J. The interface shear strength was improved after

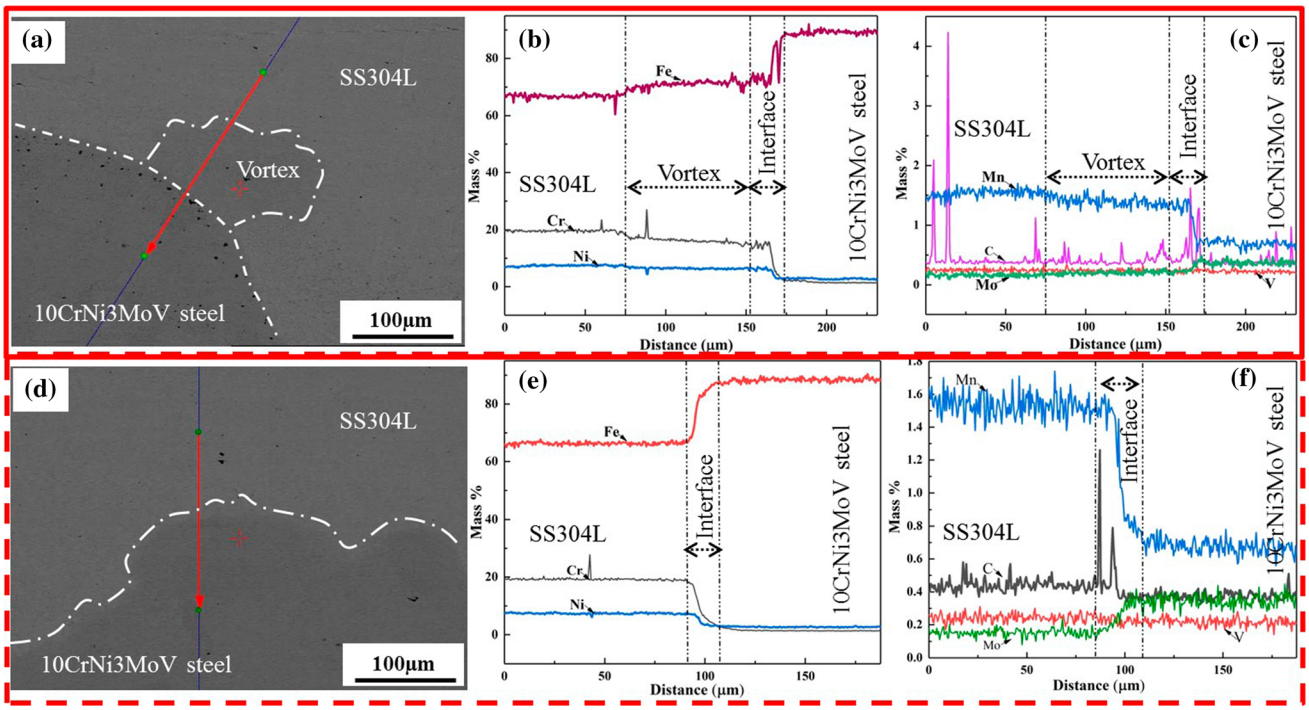

Fig. 4—SEM images and EPMA lines of the interface from the specimen that experienced one explosive welding process: (*a*) the scan line including the vortex area; (*b*) the line distribution of Fe, Cr and Ni element contents in (a); (*c*) the line distribution of Mn, C, Mo and V element contents in (a); (*d*) the scan line on the solid-solid bonding interface without a vortex; (*e*) the line distribution of Fe, Cr and Ni element contents in (d); (*f*) the line distribution of Mn, C, Mo and V element contents in (d).

Table I. Mechanical Properties of the Composite Plates

Tests Composite Plates	Fatigue Test				Impact Test	Tensile Test			Shear Test	
	Specimen No.	Loading Stress (MPa)	Fracture	Fatigue Cycles	Impact energy (J)	UTS (MPa)	YS (MPa)	EL (Pct)		Shear Strength (MPa)
Single-layer SS304L	FT-1	575	none	2×10^6	290 ± 5	688 ± 1	610 ± 1	25 ± 1		408 ± 8
	FT-2	590	none	2×10^6						
	FT-3	605	none	2×10^6						
	FT-4	620	fracture	238,739						
	FT-5	635	fracture	190,315						
Double-layer SS304L	FT-6	575	none	2×10^6	210 ± 5	687 ± 2	607 ± 2	23 ± 0	A	421 ± 2
	FT-7	590	none	2×10^6						
	FT-8	605	fracture	391,398					B	400 ± 23
	FT-9	620	fracture	84,792						
	FT-10	635	fracture	154,606						

the secondary explosive welding process. The average shear strength value of interface A (421 ± 2 MPa) was higher than that of interface B (400 ± 23 MPa). The standard deviation of the interface shear strength obtained by the secondary explosive welding process was relatively lower.

In addition, the secondary explosive welding process also reduced the fatigue performance of the material. In the single-layer SS304L composite plates, when the loading stress was > 620 MPa, the specimen fractured and the fatigue cycle was 238,739 times, while for the double-layer SS304L composite plates, when the loading stress reached 605 MPa, the fatigue specimen fractured with 391,398 cycles. Under the same loading stress of 620 MPa, the fatigue cycle of the FT-9 specimen was reduced to 84,792 times, which was only 36 pct of that of the FT-4 specimen. The fractography observation was carried out on the surface of the tested fatigue specimens as shown in Figure 5. Figures 5(a) through (d) revealed that the fatigue fracture originated from the microcracks on the surface of the specimen, and the crack propagated along the middle of the specimen until the ductile fracture was completed. The secondary explosive

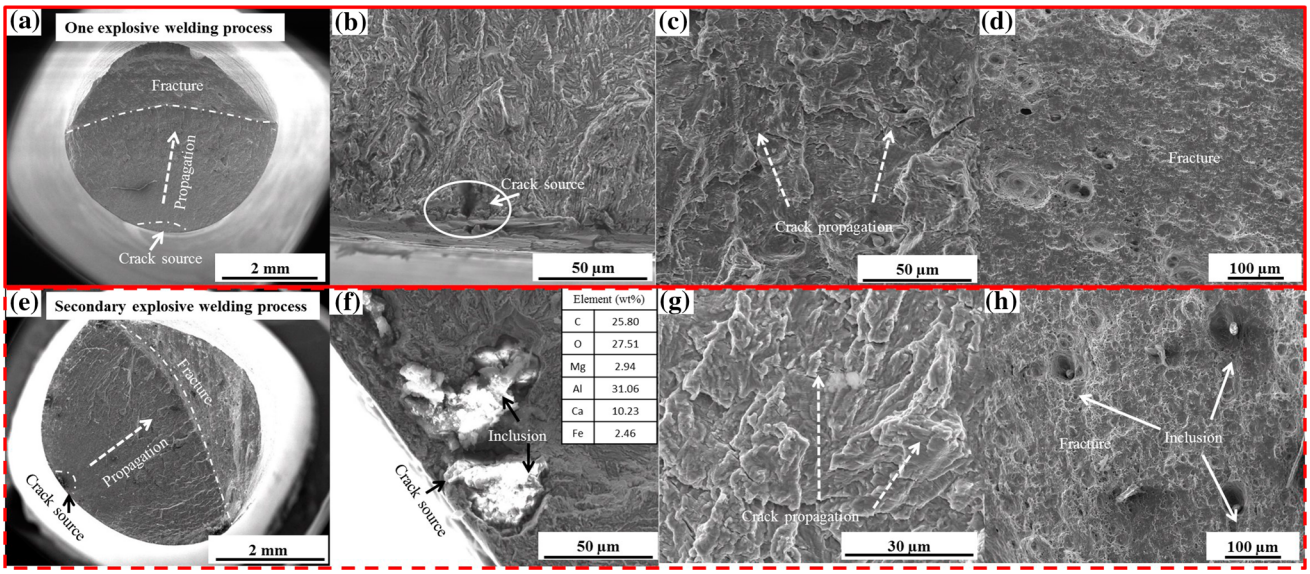

Fig. 5—Fractography of the base material 10CrNi3MoV steel after fatigue tests: (*a*) one explosive welding process; (*b*) through (*d*) crack initiation and propagation until fracture for the specimen in (a); (*e*) secondary explosive welding process; (*f*) through (*h*) crack initiation and propagation until fracture for the specimen in (e).

welding process induced the voids around inclusions to increase, and the fatigue cracks started in the inclusion area near the surface of the specimen as shown in Figures 5(e) through (h). This can be attributed to the fact that the hard and brittle phase rich in the alumina inclusion with sharp corners tended to cause a local stress concentration, which in turn formed microcracks and reduced the fatigue performance of the material.

In summary, a novel type of large-area composite plates of SS304L/10CrNi3MoV steel/SS304L sandwich structure can be prepared by the secondary explosive welding process, which can be used in industrial manufacturing. The 10CrNi3MoV steels that had undergone primary and secondary explosive welding processes all exhibited excellent low-temperature impact resistance. The impact energy was > 210 J. The shear strength of the interface increased from 400 to 421 MPa after the secondary explosive welding. The maximum load limit of the 10CrNi3MoV steel that had undergone the secondary explosive welding process was between 590 and 605 MPa when the number of loading cycles was set to 2×10^6 times.

ACKNOWLEDGMENTS

The present work was sponsored by the National Key Research and Development Program of China (grant no. 2018YFF0214702) and the Fundamental Research Funds for the Central Universities (no. 18lgpy84). The author C. Ye thanks the Postdoctoral Scientific Research Projects in Shenzhen, China.

REFERENCES

1. J. Jiang, H. Ding, Z.A. Luo, and, G.M. Xie: *J. Iron Steel Res. Int.*, 2018, vol. 25(7), pp. 732–38.
2. X. Yang, C.G. Shi, Z.H. Fang, and M.N.H. Sabuj: *Mater. Res. Express*, 2018, vol. 6(2), 026519.
3. S.V. Gladkovsky, S.V. Kuteneva, and S.N. Sergeev: *Mater. Charact.*, 2019, vol. 154, pp. 294–303.
4. F. Findik: *Mater. Des.*, 2011, vol. 32 (3), pp. 1081–93.
5. R. Mendes, J.B. Ribeiro, and A. Loureiro: *Mater. Des.*, 2013, vol. 51, pp. 182–92.
6. N. Zhang, W. Wang, X. Cao, and J. Wu: *Mater. Des.*, 2015, vol. 65, pp. 1100–09.
7. Z. Chen, D. Wang, X. Cao, W. Yang, and W. Wang: *Mater. Sci. Eng. A*, 2018, vol. 723, pp. 97–108.
8. T. Zhang, W. Wang, W. Zhang, Y. Wei, X. Cao, Z. Yan, and J. Zhou: *J. Alloys Compd.*, 2018, vol. 735, pp. 1759–68.
9. T.N. Prasanthi, C. Sudha, S. Murugesan, V.T. Paul, and S. Saroja: *Metall. Mater. Trans. A*, 2015, vol. 46A (10), pp. 4429–35.
10. B. Wronka: *J. Mater. Sci.*, 2010, vol. 45, pp. 4078–83.
11. M. Kwiecieńńn, J. Majta, and D. Dziedzic: *Arch. Civ. Mech. Eng.*, 2014, vol. 14, pp. 32–39.
12. V.I. Lysak and S.V. Kuzmin: *J. Mater. Process. Technol.*, 2015, vol. 222, pp. 356–64.
13. M.X. Xie, L.J Zhang, G.F. Zhang, J.X. Zhang, Z.Y. Bi, and P.C. Li: *Mater. Des.*, 2015, vol. 87, pp. 181–97.
14. H.B. Xia, S.G. Wang, and H.F. Ben: *Mater. Des.*, 2014, vol. 56, pp. 1014–19.
15. I.A. Bataev, A.A. Bataev, V.I. Mali, and D.V. Pavliukova: *Mater. Des.*, 2012, vol. 35, pp. 225–34.
16. C. Ye, G. Lu, L. Ni, Q. Liu, S. Hou, He. Tong, Y. Yao, and J. Zhou: *Mater. Lett.*, 2020, vol. 262, 127053.
17. N. Srinivasan, V. Kain, N. Birbilis, K.M. Krishna, S. Shekhawat, and I. Samajdar: *Corros. Sci.*, 2015, vol. 100, pp. 544–55.
18. Y. Jing, Y. Qin, X. Zeng, and Y. Li: *J. Mater. Process. Technol.*, 2014, vol. 214 (8), pp. 1686–95.
19. M. Naghizadeh and H. Mirzadeh: *Metall. Mater. Trans. A*, 2016, vol. 47A (8), pp. 4210–16.